Adsorption (2009) 15: 240–246
DOI 10.1007/s10450-009-9173-x

Effects of surface structure on the molecular projection area. Adsorption of argon and nitrogen onto defective surfaces

A contribution on the occasion of 60th birthday of Professor Mietek Jaroniec

L.F. Herrera · D.D. Do

Published online: 26 March 2009

Abstract This paper studies the effects of surface structure (defective surfaces) on the molecular projection area of argon and nitrogen at 77 K. The determination of the molecular projection area is based on choice of the surface area of the structure studied and the adsorption data obtained from the GCMC simulation. Two methods were used to determine the surface area: the flat surface area that are commonly used in the literature and the geometrical surface area. The molecular projection areas of argon and nitrogen at 77 K vary with pressure over the recommended range for BET plot (reduced pressures from 0.05 to 0.3) and also they varies with the percentage of defects on the surface. Additionally, it is seen that the geometrical surface area method gives molecular projection area of defective surfaces values that are in accordance with the experimental value reported in the literature.

Keywords Adsorption · Projection area · Simulation

1 Introduction

Traditionally, the determination of the surface area of a porous solid with adsorption methods requires the molecular projection area of the fluid molecule used (a_m) as it is one of the most important information for solid characterization (Gregg and Sing 1982; Jaroniec et al. 1999, 2003; Kowalczyk et al. 2005; Kaneko et al. 1998; Cascarini de Torre et al. 1996). Among the various probe molecules used, argon and nitrogen are the most widely used, and the recommended values for the molecular projection area of nitrogen and argon are 0.162 and 0.138 nm^2, respectively (Gregg and Sing 1982). In a recent work of Do et al. (2007) they used the Monte Carlo simulation method to investigate in details the projection area of nitrogen and argon at 77 and 87.3 K on a homogeneous graphite surface, and they found that the area occupied by one molecule varies with loading and suggested a value of 0.155 nm^2 for nitrogen and 0.128 nm^2 for argon. These values are smaller than those recommended in the literature. The reason for the difference is that they used a homogeneous graphite surface, and here we argue that the heterogeneity of the surface could affect the molecular projection area. This is the objective of this paper, and we use a recently proposed defective surface model (Do and Do 2006) as the source of heterogeneity to investigate the molecular projection area of nitrogen and argon at 77 K.

L.F. Herrera · D.D. Do (✉)
Department of Chemical Engineering, University of Queensland, St Lucia, Queensland 4072, Australia
e-mail: d.d.do@uq.edu.au

2 Theory

2.1 Fluid–fluid potential model

We model nitrogen as two Lennard Jones (LJ) dispersive sites and 3 partial charges to account for its quadrupole (Potoff and Siepmann 2001). The dispersive interaction energy between a site "a" on a molecule "i" with a site "b" on a molecule "j" is expressed by a Lennard-Jones 12-6 equation

$$\varphi_{i,j}^{(a,b)} = 4\varepsilon^{(a,b)}\left[\left(\frac{\sigma^{(a,b)}}{r_{i,j}^{(a,b)}}\right)^{12} - \left(\frac{\sigma^{(a,b)}}{r_{i,j}^{(a,b)}}\right)^{6}\right]. \quad (1)$$

Here we use the convention that the subscript is for particle while the upperscript is for site. The Lorentz-Berthelot

(LB) mixing rules are used to obtain the cross collision diameter $\sigma^{(a,b)}$ and the cross well-depth of interaction energy $\varepsilon^{(a,b)}$. Knowing the site–site interaction, the interaction between two particles can be readily computed by assuming pairwise additivity. Additionally, the interaction between a charge "α" on a molecule "i" and a charge "β" on a molecule "j" is determined via the Coulomb law of electrostatic interaction:

$$\varphi_{i,j}^{(\alpha,\beta)} = \frac{1}{4\pi\varepsilon_0} \cdot \frac{q_i^{\alpha} q_j^{\beta}}{r_{i,j}^{(\alpha,\beta)}} \tag{2}$$

where ε_0 is the permittivity of free space ($\varepsilon_0 = 8.8543 \times 10^{-12}$ $C^2\,J^{-1}\,m^{-1}$). The total electrostatic interaction between two molecules is obtained by summing all pairwise interactions.

In this potential model for nitrogen, the distance between two LJ-dispersive sites is 0.11 nm and the molecular parameters of the N-site are $\sigma = 0.331$ nm and $\varepsilon/k_B = 36$ K. Two of the three charges lie in the same positions as the two LJ-sites, and the third charge is at the center of the molecular axis joining the two LJ-sites. The charge on the LJ-site is -0.482e and the charge at the center is 0.964e.

For argon, we model it as a single LJ model with the following molecular parameters, $\sigma = 0.3405$ nm and $\varepsilon/k = 119.8$ K.

2.2 Solid–fluid potential model

The solid-fluid potential energy is calculated as the sum of all pairwise potential energies of interaction between the fluid particle i and a solid atom k as follows:

$$\varphi_{i,k} = \sum_{a=1}^{A}\sum_{b=1}^{B} 4\varepsilon_{i,k}^{(a,b)}\left[\left(\frac{\sigma_{i,k}^{(a,b)}}{r_{i,k}^{(a,b)}}\right)^{12} - \left(\frac{\sigma_{i,k}^{(a,b)}}{r_{i,k}^{(a,b)}}\right)^{6}\right] \tag{3}$$

where $\varphi_{i,k}$ is the interaction energy between fluid molecules i and the solid atom k, A and B are the number of LJ sites on molecule i and the solid, respectively, and $r_{i,k}^{(a,b)}$ is the distance between the LJ site a on molecule i and site b on the solid atom k. The LJ parameters between the fluid and the carbon atom are calculated using the Lorentz-Berthelot mixing rules with $\varepsilon_k/k_B = 28$ K and $\sigma_k = 0.34$ nm for the carbon atoms in the graphene layer.

2.3 Monte Carlo simulation

The surface structure is created by a series of three graphene layers, with only the surface layer defective. The surface structure is placed at the bottom of the simulation box (Fig. 1). The simulation box is rectangular in shape with height (H), length (L) and width (W) equal to 4 nm, 4.6 and 4.4 nm, respectively.

To develop the defective surface layer, there are different approaches, such as the model proposed by Turner and Quirke in 1998. They proposed that defective graphite layer can be constructed by removing benzene rings from the surface layer. In this work the defective layer is constructed by using the method proposed in the literature (Do and Do 2006). The defects can be created by selecting a carbon atom at random and then removing it together with neighbouring carbon atoms within a distance less than an effective defect radius R (here we choose $R = 0.492$ nm). Five different percentages of defects were used (0, 10, 20, 30, and 50%) and these layers are shown in Fig. 2.

The Monte Carlo simulations were performed using the GCMC ensemble. The adsorption isotherms of nitrogen and argon were obtained at 77 K. The saturation vapour pressures of nitrogen and argon are 101.33 and 21.5 kPa, respectively. The chemical potentials used in the simulations were the ideal chemical potentials at the pressures reported. Each isotherm point was equilibrated using 7×10^6 attempted trial moves while the ensemble averages was calculated with 5×10^6 trial moves. Each trial move consists of moves (ei-

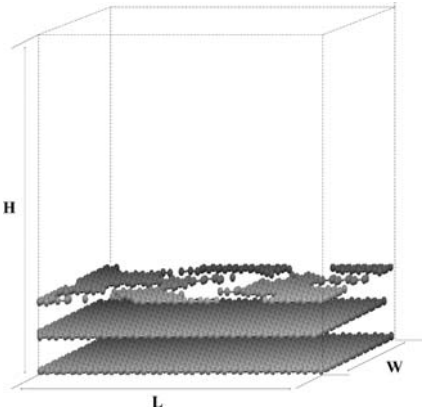

Fig. 1 Simulation box with graphene layers at the bottom. The outermost graphene layer is made defective with a defect percentage and a defect radius

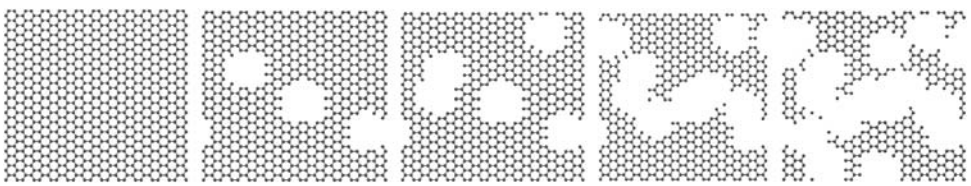

Fig. 2 Carbon layer placed on the top with percentage of defects of 0, 10, 20, 30 and 50% from left to right

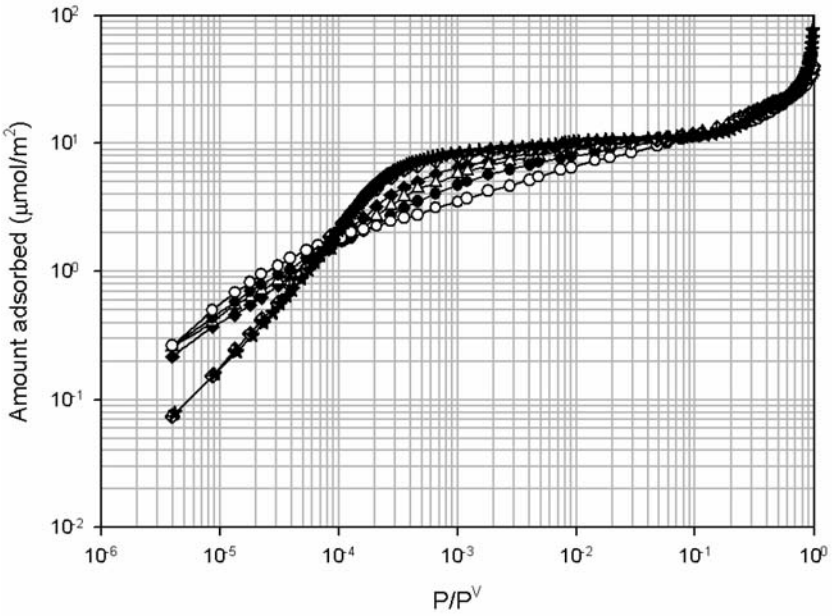

Fig. 3 Adsorption data for nitrogen at 77 K on studied surfaces. (★) Experimental data from Kruk et al. GCMC simulation results of surfaces with (—◈—) no defects, (—◆—) 10, (—△—) 20, (—●—) 30 and (—○—) 50% of defects. Data calculated based on the flat surface area

ther a rotation or translation), insertions and deletions. Additionally, periodic boundary conditions are applied in the x and y-directions while the top boundary in the z-direction is treated as a hard wall. Also during the course of simulation, the minimum distance between a fluid molecule and the solid was recorded, from which the average numbers of particles in the first and higher layers were determined.

3 Simulation results

From the GCMC simulation, we obtain the ensemble average of the number of particle at a given chemical potential. To calculate the surface concentration (μmol/m^2), we use two different surface areas. One is the area based on the assumption of a flat surface, and therefore the surface area is $A = LW = 20.24$ nm^2. The other area is the actual geometrical surface area, which is calculated as follows. For each solid atom, the possible surface area is the area of a sphere of radius σ_{sf} having the same centre as the centre of the solid atom. Therefore for N solid atoms in the simulation box, the total possible surface area is $A = 4\pi(\sigma_{sf})^2 N$. However, not all that area is available for adsorption because of the overlapping of those spheres with neighbouring solid atoms. To calculate the fraction of that spherical area that is available for adsorption, we carry out the Monte Carlo integration to obtain the fraction for a solid atom j as F_j. Thus the geometrical area is $A = 4\pi(\sigma_{sf})^2 \sum_{j=1}^{N} F_j$. Because of the defects and the intrinsic roughness the geometrical area is greater than the flat surface area. We obtain the following values for the geometrical surface area 20.88, 22.01, 22.63, 23.89, and 25.59 nm^2 for surfaces of 0, 10, 20, 30 and 50% of defects on the surface, respectively.

3.1 Nitrogen

The adsorption isotherms of nitrogen on defective surfaces at 77 K, using the flat surface area, are shown in Fig. 3. The GCMC simulation results for the surface with no defect agree well with the experimental adsorption data of nitrogen on highly graphitized thermal carbon black (Kruk et al. 1999). For surfaces with defects we do not observe the Henry law region because the slope of the isotherm is less than unity. This is due to the fact that adsorption occurs on the highest energy site first and then progresses to sites of decreasing energy. Because of the same reason, we see that adsorption on the defective surfaces is greater than that on perfect surface. Furthermore the packing of adsorbed molecules on defective surfaces is not well ordered (Cascarini de Torre et al. 1996; Herrera et al. 2008), and as a result each molecule will occupy a larger area than in the case of a perfect surface.

The nitrogen adsorption isotherm calculated based on the geometrical surface area is presented on Fig. 4. The behaviours of these isotherms are similar to what we have seen earlier with the flat surface area calculation. The only difference is that the loadings are lower because of the larger geometrical surface area compared to the flat surface area.

The adsorption isotherm provides us information on the amount adsorbed at a given chemical potential. To investigate how molecules position themselves above the surface, we need to determine the local density distribution. For a well defined surface such as flat surface or smooth cylindrical surface, it is simple to divide the space above the surface into bins of equal size and during the course of simulation we keep track of the number of particle in each bin. At the end of the simulation, the ensemble averages of all bins are

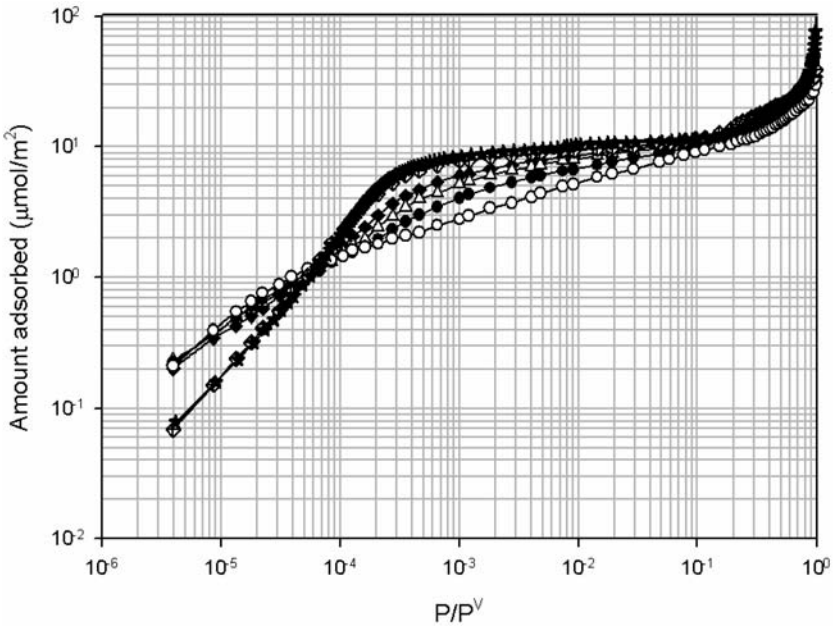

Fig. 4 Nitrogen adsorption data at 77 K on studied surfaces. (★) Experimental data from Kruk et al. GCMC simulation results of surfaces with (—◈—) no defects, (—◆—) 10, (—△—) 20, (—●—) 30 and (—○—) 50% of defects. Data calculated based on the geometrical surface area

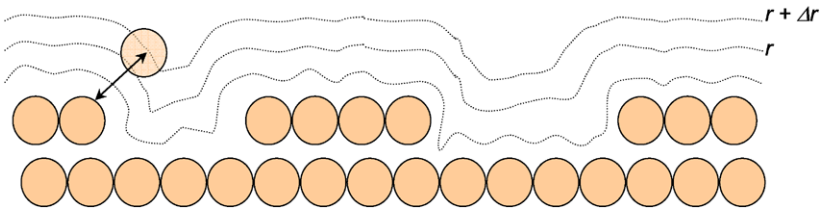

Fig. 5 Schematic diagram of the number of particles distribution determination

obtained and this gives the local density with respect to distance. However, for irregular surfaces that we deal with here, such an approach is not appropriate. For a defective surface, we perform this as follows. For each particle in the simulation box, we calculate its shortest distance from the surface, and if this distance is between r' and $r' + \Delta r'$ the bin "r'" having a thickness of $\Delta r'$ is incremented by one. This process is repeated for all particles. Once the simulation has been completed we simply obtain the ensemble average of each bin. The contour of equi-distance from the surface is shown schematically in Fig. 5.

Figure 6 shows the number of particles versus the shortest distance for nitrogen adsorption at 77 K on defective surfaces of various defect percentages. We do this for the range of reduced pressure between 0 and 0.3. Here, we can see clearly the disorganized structure of adsorbed phase for the surfaces with high defect. This is reflected in the significant overlapping between the first and second layers (see Fig. 6e).

Having the distribution of local density with respect to the shortest distance, we can calculate the number of molecules in the first layer, i.e. we count only molecules that are in close contact with the surface. These molecules are said to be confined in the first layer adjacent to the surface. The monolayer concentration is then simply the ratio of the number of molecules in the first layer to the surface area. The area used can be either the flat surface area or the geometrical surface area. The molecular projection area is then the inverse of the monolayer concentration. The results for the molecular projection area with the flat surface area and the geometrical surface area are shown in Figs. 7a and 7b, respectively. For the case of the molecular projection area calculated with the flat surface, Fig. 7a shows that for reduced pressures less than 0.095 the molecular projection area decreases with the percentage of defects, but this effect is reverse for reduced pressures between 0.095 and 0.3. On the other hand, Fig. 7b shows the molecular projection area calculated with the geometrical surface area increases with the percentage of defects, irrespective of the reduced pressure.

Having the molecular projection area as a function of reduced pressure as shown in Fig. 7, the average molecular projection area can be calculated from

$$\langle a_m \rangle = \frac{1}{x_2 - x_1} \int_{x_1}^{x_2} a_m dx \tag{4}$$

where x is the reduced pressure, x_2 and x_1 are the low and high reduced pressure limits according to BET theory (Gregg and Sing 1982) (0.05 and 0.3) and a_m is the molecular projection area. The average projection area calculated for all surfaces are presented in Fig. 8. The figure also

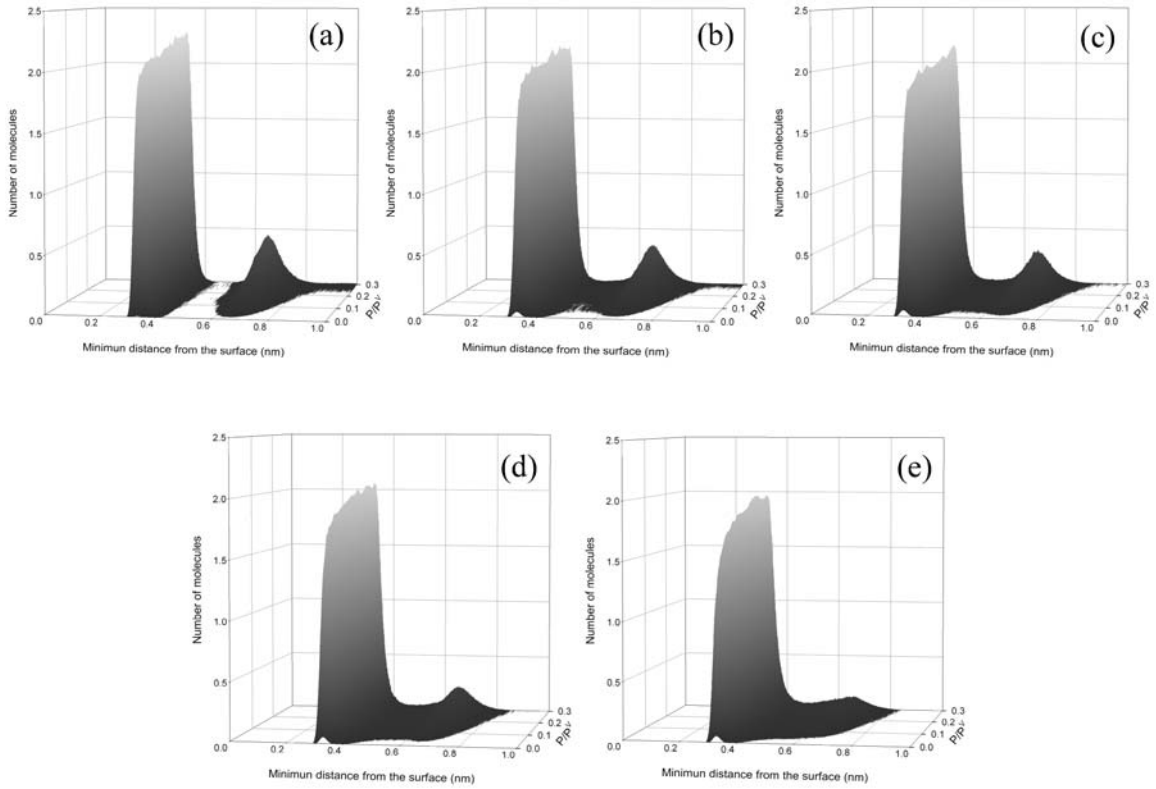

Fig. 6 Number of particles distribution of nitrogen at 77 K: (**a**) no defective surface, (**b**–**e**) surfaces with 10, 20, 30 and 50% of defects

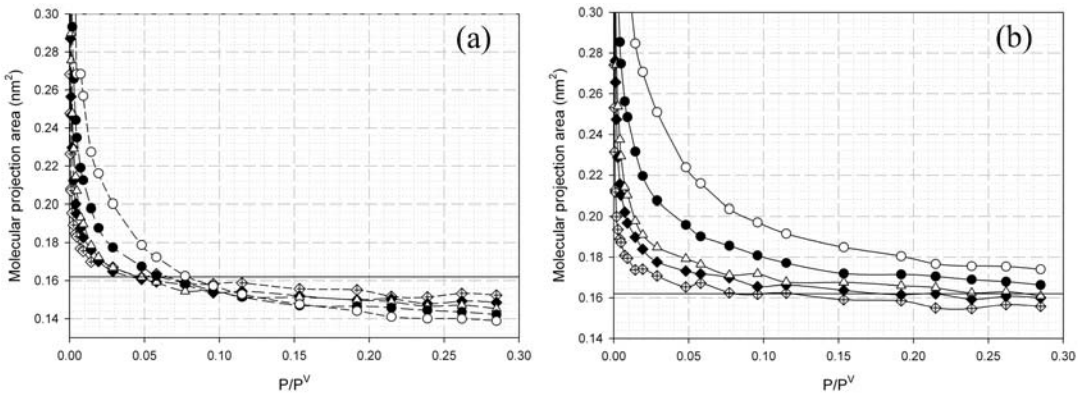

Fig. 7 Molecular projection area of nitrogen against reduced pressure for surfaces with (–◈–) no defects, (–◆–) 10, (–△–) 20, (–●–) 30 and (–○–) 50% of defects. Surface area calculated as a flat surface (**a**) and with the geometrical surface area (**b**). The *horizontal line* indicates the molecular projection area calculated with nitrogen as a liquid at 77 K (0.162 nm)

shows the lowest (0.141 nm) and highest (0.277 nm) limits (dashed lines) found by Arnell and Henneberry (1948) from the experimental determination over 11 different carbon black samples and the commonly used molecular projection area of 0.162 nm^2 (solid horizontal line).

Figure 8 shows that for all cases the average molecular projection area is between the lower and upper limits calculated by Arnell and Henneberry (1948). Additionally, all molecular projection areas calculated with the flat surface assumption show a lower value than the value recommended in the literature (0.162 nm^2). In contrast, only the data calculated with the geometrical surface area for the perfect graphite surface is lower than 0.162 nm^2. The larger values obtained using the geometrical surface area for defective surfaces seemed to support the common value of 0.162 nm^2, and it suggests that this value is applicable for heterogeneous surfaces and it is borne in mind that for highly heterogeneous surfaces the molecular projection area greater

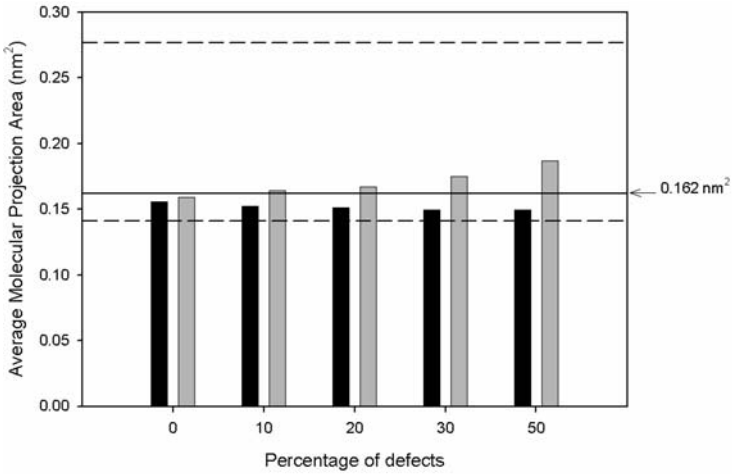

Fig. 8 Average molecular projection area for nitrogen on surfaces with different percentages of defects. *Black bars* indicate the surface area calculated as a flat surface while the *gray bars* are calculated with the geometrical surface area. The *horizontal dashed lines* indicates the lowest (0.141 nm^2) and highest (0.277 nm^2) cross section areas while the *continuous line* is the common value used of 0.162 nm^2

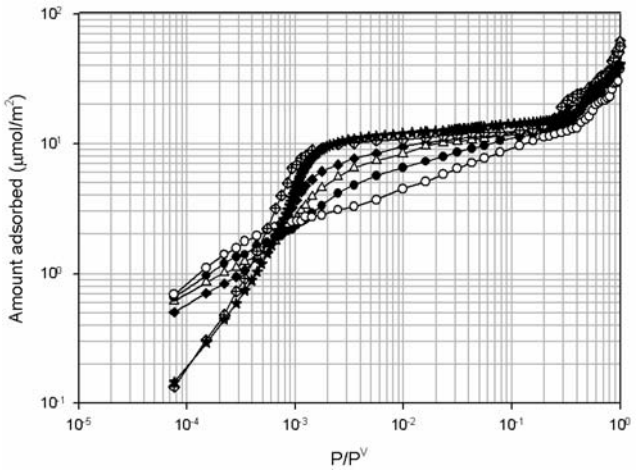

Fig. 9 Argon adsorption data at 77 K on the surfaces studied. (★) Experimental data from Gardner et al.. GCMC simulation results of surfaces with: (—◈—) no defects, (—◆—) 10, (—△—) 20, (—●—) 30 and (—○—) 50% of defects. Data were calculated based on the geometrical surface area

than 0.162 nm^2 should be used instead (see the value for a defective surface with 50% defect in Fig. 8).

3.2 Argon

Beside nitrogen, argon is often used as a probe particle for porous solid characterization, and in some cases it is a preferred adsorptive because it is spherical and does not have a quadrupole. The adsorption isotherms of argon at 77 K on defective surfaces with different percentages of defects are shown in Fig. 9. Here we use the geometrical surface area in the calculation of the amount adsorbed. Like the case of nitrogen, the Henry law region is not observed for surfaces having defects over the pressure range studied here.

From the knowledge of the density distribution we calculate the molecular projection area using the geometrical surface area, and the results are shown in Fig. 10. What we have seen earlier with nitrogen is repeated here with argon, that is the molecular projection area is not constant. It varies with pressure and with the degree of heterogeneity of the surface.

The average molecular projection areas for all cases studied are presented in Fig. 11. The recommended value for a homogeneous graphite surface is 0.1294 nm^2 (Gregg and Sing 1982) is shown in the same figure as the horizontal solid line. It is seen that the areas obtained for defected surfaces, using either the flat surface area or the geometrical surface area, are higher than the value used for a homogeneous graphite surface and they also are higher than the value recommended for argon of 0.138 nm^2 (Gregg and Sing 1982), that is commonly used in the literature. For highly defected surfaces, such as the 50% defective surface the molecular projection area is as high as 0.17 nm^2. Thus it is important to recognize this in the use of the recommended value of 0.138 nm^2. If the given surface is known to be very heterogeneous, then the surface area calculated with the common value of 0.138 nm^2 could underestimate the real geometrical value.

4 Conclusions

In this paper, the molecular projection areas of nitrogen and argon at 77 K on defective surfaces were obtained by using the GCMC simulation method. We determine the projection area by using the flat surface area and the geometrical surface area. The projection area using the latter, in general, agrees better with the value recommended for nitrogen and argon when applied to practical solids. However, it should be noted that the molecular projection area is not constant over the recommended range for BET plot of 0.05 to 0.3

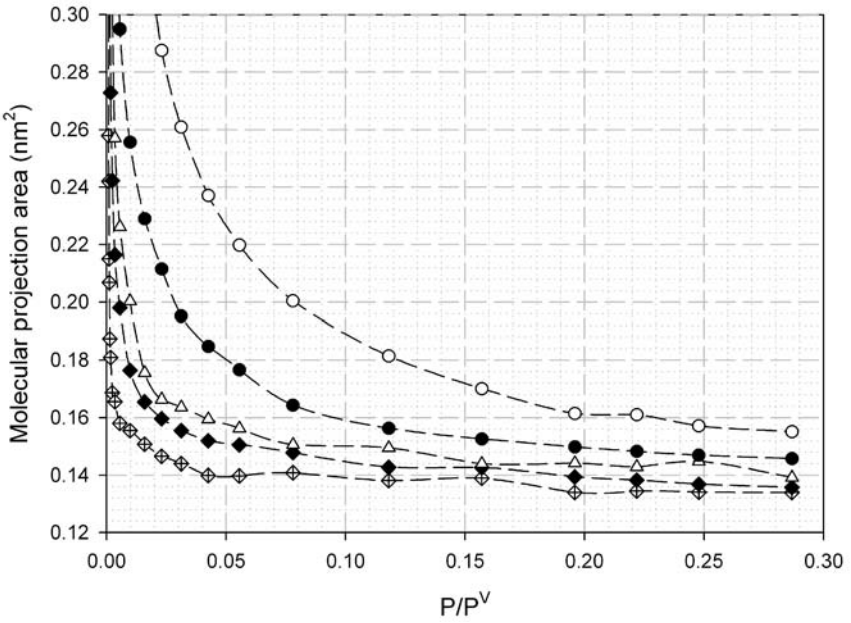

Fig. 10 Molecular projection area of argon against reduced pressure for surfaces with (—◈—) no defects, (—◆—) 10, (—△—) 20, (—●—) 30 and (—○—) 50% of defects. Surface area is the geometrical surface area

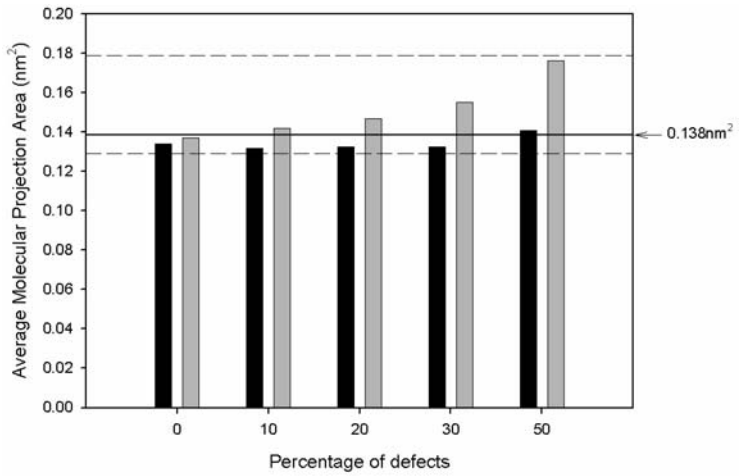

Fig. 11 Average molecular projection area for argon on surfaces with different percentages of defects. *Black bars* indicate the surface area calculated as a flat surface while the *gray bars* are calculated with the geometrical surface area. The *horizontal line* is the constant value of 0.138 nm^2 recommended for graphite in the literature

in reduced pressure. Furthermore, it also varies with the degree of heterogeneity. For example, with the defective surface model that we employed here, the molecular projection area of nitrogen varies between 0.159 to 0.187 nm^2 for surface defect percentage ranging between 0 and 50%. For the case of argon the projection area varies between 0.137 and 0.176 nm^2 for the same set of surfaces. Even with a simple model of heterogeneous surface that was used in this paper, the molecular projection area has a wide variation. Therefore one could conjecture that with practical solids with high degree of heterogeneity and with chemical heterogeneity the molecular projection area could have even a wider range. This supports the wide range of values reported by Arnell and Henneberry in their survey of molecular projection area.

Acknowledgement This project is supported by the Australian Research Council.

References

Arnell, J.C., Henneberry, G.O.: Can. J. Res. **26A**, 29–38 (1948)
Cascarini de Torre, L.E., Bottani, E.J., Steele, W.A.: Langmuir **12**, 533–5406 (1996)
Do, D.D., Do, H.D.: J. Phys. Chem. B **110**, 17531–17538 (2006)
Do, D.D., Do, H.D., Nicholson, D.: Adsorpt. Sci. Technol. **25**, 347–363 (2007)
Gregg, S., Sing, K.: Adsorption and Porosity. Academic Press, New York (1982)
Herrera, L.F., Do, D.D., Birkett, G.R.: J. Colloid Interface Sci. **320**, 415–422 (2008)
Jaroniec, M., Choma, J., Kruk, M.: Colloids Surf. A **214**, 263–269 (2003)
Jaroniec, M., Kruk, M., Olivier, M.: Langmuir **15**, 5410–5413 (1999)
Kaneko, K., Ishii, C., Kanoh, H., Hanzawa, Y., Setoyama, N., Suzuki, T.: Adv. Coll. Int. Sci. **76**, 295–320 (1998)
Kowalczyk, P., Jaroniec, M., Terzyk, A., Kaneko, K.: Langmuir **21**, 1827–1833 (2005)
Kruk, M., Li, Z., Jaroniec, M.: Langmuir **15**, 1435–1441 (1999)
Potoff, J.J., Siepmann, J.I.: AIChE Journal **47**, 1676–1682 (2001)
Turner, A.R., Quirke, N.: Carbon **36**, 1439–1446 (1998)